Reconstruction in Diffraction Ultrasound Tomography Using Non-Uniform FFT

Michael BRONSTEIN, Alexander BRONSTEIN and Michael ZIBULEVSKY

***Abstract*--We show an iterative reconstruction framework for diffraction ultrasound tomography. The use of broadband illumination allows significantly reduce the number of projections compared to straight ray tomography. The proposed algorithm makes use of forward non-uniform fast Fourier transform (NUFFT) for iterative Fourier inversion. Incorporation of total variation regularization allows reduce noise and Gibbs phenomena whilst preserving the edges.**

***Index Terms*--acoustic tomography, image reconstruction, nonuniform FFT.**

I. Introduction

Ultrasound tomography with diffracting sources is an important type of acoustic imaging. Since the used wavelengths are comparable to the object feature dimensions, wave phenomena such as diffraction become significant. Consequently, the straight ray tomography theory is no more applicable.

The analog of the Fourier Slice Theorem used in straight ray tomography is the Fourier Diffraction Theorem [1]. Using this theorem, image reconstruction in diffraction tomography can be considered as a problem of signal reconstruction from non-uniform frequency samples.

Reconstruction methods used beforehand addressed the problem as straightforward approximation of the inverse non-uniform Fourier transform (NUFT) and involved frequency interpolation [1], which is liable to introduce significant inaccuracies. More accurate and computationally efficient methods [2]-[5] were proposed for forward and inverse 1D NUFT. Fast forward NUFT algorithms can be generalized to higher dimensions, whereas the generalization of the inverse ones is not trivial. For this reason, we limit our work to the use of the forward NUFFT.

Recently, fast and accurate approximation of the forward NUFFT was introduced by Fessler and Sutton [6]. Inverse NUFFT can be achieved iteratively in this framework [7]. We adopt this approach for iterative reconstruction in diffraction tomography, combining it with total variation regularization [8]-[10] in order to suppress noise preserving the sharpness of edges.

Simulation studies with the Shepp-Logan phantom show that the proposed algorithm significantly outperforms the frequency interpolation methods.

Manuscript received March 8, 2002. This research has been supported in part by the Ollendorff Minerva Center, by the Fund for Promotion of Research at the Technion, and by the Israeli Ministry of Science.

M. Bronstein (e-mail: bron@tx.technion.ac.il), A. Bronstein (e-mail: bron@aluf.technion.ac.il) and M. Zibulevsky (e-mail: mzib@ee.technion.ac.il) are with the Technion – Israel Institute of Technology, Department of Electrical Engineering, Haifa 32000, Israel.

II. Principles of Diffraction Tomography

Tomography is a method of obtaining an image of a slice of the object from projections. A projection is obtained by illuminating the object from a certain angle and measuring the traversing radiation. In diffraction ultrasound tomography, the object is illuminated with a plane acoustic wave. The forward scattered field is measured on a line of detectors, as shown in Figure 1. As in straight ray tomography, changing the orientation of the incident plane waves, it is possible to acquire projections at different angles. Unlike conventional tomography, incident wave frequency can also be changed.

When the wavelength of the incident wave is of the same order as the typical feature size, wave phenomena cannot be neglected. Particularly, diffraction has a significant effect on the interaction of the radiation with matter, and the model of line integrals and the Radon transform is not applicable in diffraction tomography.

Reconstruction is possible by the solution of the inverse problem. Unlike straight ray tomography, the preferable strategy is the solution of the inverse problem in frequency domain. Under the assumption of weakly scattering inhomogeneities in the object, the Fourier Diffraction Theorem relates the Fourier transform of the measured scattered field projection with the Fourier transform of the object:

The Fourier Diffraction Theorem

Given a projection $P_\theta(r)$ of the forward scattered field (θ denotes the projection angle and r is the radius) obtained by illuminating an object $f(x,y)$ with a plane wave as shown in Figure 1, the following equation holds:

$$\mathcal{F}\{P_\theta(r)\}(\omega) = \mathcal{F}_{2D}\{f(x,y)\}\left(K_x(\omega), K_y(\omega)\right) \qquad (1)$$

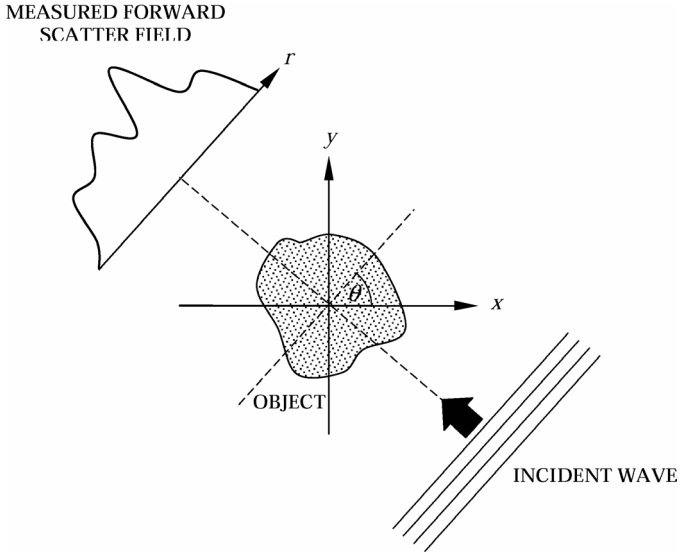

Fig. 1. Acquisition of a single projection in ultrasound diffraction tomography [1].

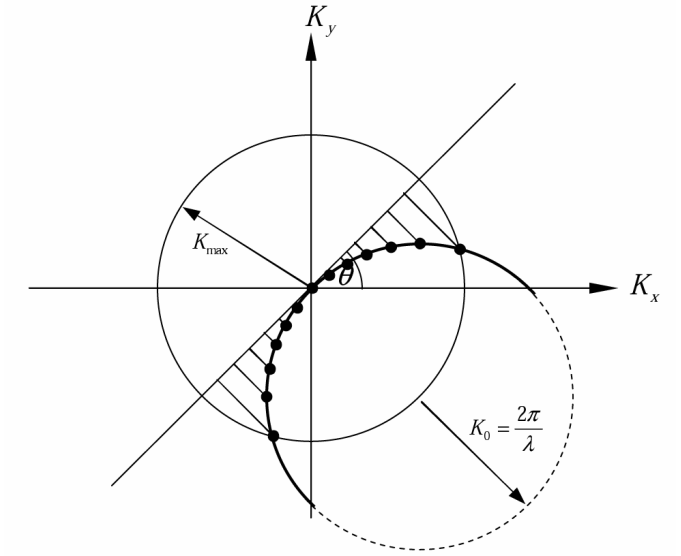

Fig. 2. Illustration of the Fourier Diffraction Theorem.

where

$$K_x(\omega) = \omega\cos\theta - \left(\sqrt{K_0^2 - \omega^2} - K_0\right)\sin\theta,$$
$$K_y(\omega) = \omega\sin\theta + \left(\sqrt{K_0^2 - \omega^2} - K_0\right)\cos\theta, \qquad (2)$$
$$K_0 = \frac{2\pi}{\lambda},$$

λ is the wavelength and $\mathcal{F}$ and $\mathcal{F}_{2D}$ denote the one- and two-dimensional Fourier transforms, respectively.

In other words, the Fourier transform of the projection gives the values of the 2D Fourier transform of the object along a semi-circular arc in the spatial frequency domain, as depicted in Figure 2. For proof see, for example, Kak and Slaney [1].

One can note that the arc radius becomes large as the wavelength shortens and the Diffraction Theorem approaches the Slice Theorem.

Since wave phenomena obey the superposition principle, illuminating the object with a wave consisting of a set of frequencies (referred to as *broadband illumination*), rather than a monochromatic wave, will produce samples along a set of semi-circular arcs with different radii. Hence, a single projection potentially contains much more information about the object than a single projection in straight ray tomography. By taking advantage of this fact, one can achieve sufficient image quality with fewer projections.

Two main reconstruction strategies in diffraction tomography are interpolation in frequency domain (analogous to the direct Fourier inversion in straight ray tomography) and interpolation in space domain (analogous to the filtered backprojection), usually termed as *backpropagation*. However, unlike straight ray tomography, interpolation in space domain is computationally extensive, and thus the majority of efficient algorithms are based on frequency domain interpolation.

A common way for image reconstruction in frequency domain is the gridding algorithm [1],[11]. The non-uniform data is interpolated to a uniform Cartesian grid using, for example, polynomial interpolation. Afterwards, the inverse Fourier transform is efficiently computed using FFT. However, this approach is liable to introduce inaccuracies and is sensitive to the configuration of the sample points.

In the next part, we introduce an iterative reconstruction method, which allows reconstruct the image from non-uniform samples in frequency domain without using gridding.

III. Non-Uniform Fourier Transform

The heart of iterative image reconstruction from non-uniform frequency samples is the forward non-uniform fast Fourier transform. To define the NUFFT problem, we first consider a one-dimensional case.

Let $\boldsymbol{\xi} = (\xi_1, ..., \xi_N) : \xi_k \in [-\pi, \pi]$ be a vector of non-uniformly distributed frequencies and $\boldsymbol{f} = (f_{-N/2}, ..., f_{N/2-1}) : f_n \in \mathbb{C}$ be a vector of samples of a signal. The non-uniform Fourier transform is defined by the formula

$$F_k = \sum_{n=-N/2}^{N/2-1} f_n \exp(-ik\xi_k) \qquad (3)$$

In matrix notation

$$\boldsymbol{F} = \Psi\boldsymbol{f} \qquad (4)$$

where $\Psi \in \mathbb{C}^{K\times N}$ ($K \geq N$) is a full column rank matrix containing K discrete exponent functions in its rows

$$\Psi = (\boldsymbol{\psi}_1; ...; \boldsymbol{\psi}_K) \;;\; \boldsymbol{\psi}_k(n) = \exp(-in\xi_k) \qquad (5)$$

Fast approximation $\mathcal{T}$ of the NUFT operator can be achieved by projecting the signal $\boldsymbol{f}$ on some oversampled uniform Fourier basis $\Phi \in \mathbb{C}^{qN\times N}$ using standard FFT, with consequent efficient interpolation:

$$\boldsymbol{F} \approx \mathcal{T}\boldsymbol{f} = \mathrm{U}_p\Phi\boldsymbol{f} \qquad (6)$$

where U_p denotes the interpolation operator, which makes use of p neighboring uniform samples for approximation of each non-uniform sample. The overall complexity of such an algorithm is $O(qN \log qN + pK)$.

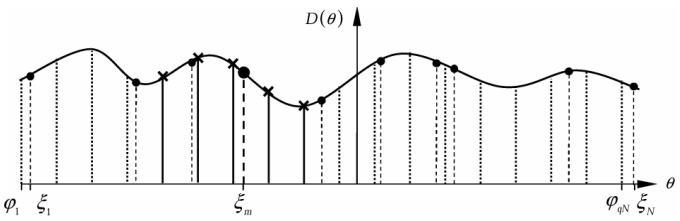

Fig. 3. Example of 1D forward NUFFT using p neighbors: Discrete Time Fourier Transform $D(\theta)$ of the signal (solid line), is sampled at qN uniform points (dotted lines). Transform value in the non-uniform grid point ξ_m (large dot) is approximated using p uniform neighbors (crosses).

Fessler and Sutton [6],[7] proposed obtaining such interpolation coefficients that minimize the maximum approximation error at a given point of the non-uniform grid over all signals with unit l_2-norm. This approach can be formulated as a min-max problem:

$$\min_{\boldsymbol{u}_k} \max_{\|\boldsymbol{f}\|_2 \le 1} \left| \boldsymbol{u}_\kappa \Phi_p^k \boldsymbol{f} - \boldsymbol{\psi}_\kappa \boldsymbol{f} \right|^2 \tag{7}$$

where $\boldsymbol{u}_k$ is the non-zero part of the k-th row of the interpolation matrix U_p and Φ_p^k is a part of the overcomplete DFT basis Φ, containing p nearest neighbors of the non-uniform basis element $\boldsymbol{\psi}_k$.

Substituting explicit expression for the maximum

$$\max_{\|\boldsymbol{f}\|_2 \le 1} \left| \left(\boldsymbol{u}_k \Phi_p^k - \boldsymbol{\psi}_k \right) f \right|^2 = \left\| \boldsymbol{u}_k \Phi_p^k - \boldsymbol{\psi}_k \right\|_2^2, \tag{8}$$

problem (7) is reduced to the following least-squares formulation:

$$\min_{\boldsymbol{u}_k} \left\| \boldsymbol{u}_k \Phi_p^k - \boldsymbol{\psi}_k \right\|_2^2, \tag{9}$$

which has an analytic solution:

$$\boldsymbol{u}_k = \boldsymbol{\psi}_\kappa \Phi_p^{k\mathrm{H}} \left(\Phi_p^k \Phi_p^{k\mathrm{H}} \right)^{-1} \tag{10}$$

corresponding to the coefficients of the best approximation of $\boldsymbol{\psi}_k$ in Φ_p^k. In practice, the interpolation coefficients can be pre-computed. One of the advantages of the min-max approach is the fact that it allows efficient computation of the adjoint operator, crucial for iterative optimization algorithms.

IV. Iterative Solution of The Inverse Problem

A. Formulation of the optimization problem

Straightforward solution of the inverse problem of (4) is a computationally extensive operation. It is given by the Moore-Penrose pseudoinverse:

$$\boldsymbol{f} = \Psi^+ \boldsymbol{F} = \left(\Psi^{\mathrm{H}} \Psi \right)^{-1} \Psi^{\mathrm{H}} \boldsymbol{F} \tag{11}$$

Alternatively, equation (4) can be reformulated as an optimization problem:

$$\min_{\boldsymbol{f}} \left\| \mathcal{T} \boldsymbol{f} - \boldsymbol{F} \right\|_2^2 \tag{12}$$

It is possible to add penalty on some kind of signal irregularity to the object function:

$$\min_{\boldsymbol{f}} \left\| \mathcal{T} \boldsymbol{f} - \boldsymbol{F} \right\|_2^2 + \lambda \varphi(\boldsymbol{f}) \tag{13}$$

where λ is a parameter controlling the influence of the penalty. This problem can be solved iteratively using various optimization techniques, like Conjugate Gradients, Truncated Newton, etc. (see, for example [12]). They require efficient computation of the objective function and its gradient, which use in turn fast forward operator $\mathcal{T}$, and its adjoint $\mathcal{T}^\dagger$. The gradient of the cost function $g(\boldsymbol{f})$ in (13) is given by

$$\nabla g(\boldsymbol{f}) = 2\mathcal{T}^\dagger \left(\mathcal{T} \boldsymbol{f} - \boldsymbol{F} \right) + \nabla \varphi(\boldsymbol{f}) \tag{14}$$

B. Total variation regularization

Empirical observations show that the majority of images that occur in nature, and particularly in medical imaging applications, belong to the class of functions of bounded total variation (defined as the integral of the gradient l_2-norm) [13].

The penalty term for total variation can be used in problem (13). For discrete image, the total variation is given by

$$\sum_{i,j} \sqrt{\left(\boldsymbol{f}_x \right)_{ij}^2 + \left(\boldsymbol{f}_y \right)_{ij}^2} \tag{15}$$

where $\boldsymbol{f}$ is the estimated discrete image being found during the iterative process and $\boldsymbol{f}_x$, $\boldsymbol{f}_y$ are its discrete directional derivatives.

Since this function is not smooth, which can be an obstacle for smooth optimization techniques, adding a positive smoothing parameter η, we finally get the smoothed total variation penalty:

$$\varphi(\boldsymbol{x}) = \sum_{i,j} \sqrt{\left(\boldsymbol{f}_x \right)_{ij}^2 + \left(\boldsymbol{f}_y \right)_{ij}^2 + \eta} \tag{16}$$

The gradient of the total variation penalty term is given by

$$\nabla_{f_{i,j}} \varphi = \lambda \left[\varphi_{i-1,j}^x - \varphi_{i,j}^x - \varphi_{i,j}^y + \varphi_{i,j-1}^y \right], \tag{17}$$

where

$$\begin{aligned} \varphi_{i,j}^x &= \frac{\left(\boldsymbol{f}_x \right)_{i,j}}{\sqrt{\left(\boldsymbol{f}_x^2 \right)_{i,j} + \left(\boldsymbol{f}_y^2 \right)_{i,j} + \eta}} \\ \varphi_{i,j}^y &= \frac{\left(\boldsymbol{f}_y \right)_{i,j}}{\sqrt{\left(\boldsymbol{f}_x^2 \right)_{i,j} + \left(\boldsymbol{f}_y^2 \right)_{i,j} + \eta}} \end{aligned} \tag{18}$$

Total variation regularization removes small oscillations (resulting from noise and Gibbs phenomena), without significantly affecting the edges.

V. SIMULATIONS

A. Shepp-Logan phantom

In order to avoid forward-projection errors, we used an analytic Shepp-Logan phantom. This phantom is a superposition of ellipses representing features of the human brain. The advantage of such phantom is that its Fourier transform has a simple analytical expression. Fourier transform of an ellipse centered at $\left(x^0, y^0\right)$, with intensity ρ, lengths of horizontal and vertical semi-axes A and B, respectively and orientation α is given by:

$$E\left(K_x, K_y\right) = \rho e^{-i\left(K_x x^0 + K_y y^0\right)} \frac{AJ_1\left(B\sqrt{\left(u'AB^{-1}\right)^2 + v'^2}\right)}{\sqrt{\left(u'AB^{-1}\right)^2 + v'^2}}, \quad (19)$$

where $u' = K_x \cos\alpha + K_y \sin\alpha$ and $v' = -K_x \sin\alpha + K_y \cos\alpha$ and J_1 is the first-order Bessel function of the first kind. Fourier transform of the entire phantom is expressed by

$$F\left(K_x, K_y\right) = \sum_{k=1}^{N} E\left(K_x, K_y; \rho_k, x_k^0, y_k^0, A_k, B_k, \alpha_k\right) \quad (20)$$

Eight simulated broadband projections (each containing 10 frequencies) are shown in Figure 4. For comparison, in similar conditions, a conventional filtered backprojection (FBP) would require about 100 straight ray projections for good reconstruction of a 64×64 image [14].

B. Comparison between gridding and iterative reconstruction

The standard gridding algorithm [1] involving frequency interpolation was compared to iterative reconstruction. Non-uniform frequency samples were interpolated on a 64×64 uniform Cartesian grid and then inverted by IFFT.

Fessler's NUFFT algorithm, given by (6) and (10) was used as the forward operator in iterative reconstruction[1]. Solution of the optimization problem was performed using Conjugate Gradients.

Figure 5 depicts the reconstruction results. It can be seen that unlike iterative reconstruction, the use of gridding introduces significant artifacts. Interpolation in frequency domain appears to be highly sensitive to the distribution of the frequency samples.

Figure 6 reveals that regridding the non-uniformly spaced data to a Cartesian grid suffers from inaccuracies. Iterative reconstruction appeared to be more accurate than gridding. RMS error in frequency domain of the iterative algorithm (with respect to the analytic phantom) was about 5 times lower compared to gridding.

C. The influence of total variation regularization

Tests were performed to study the influence of total variation regularization. Figure 5 shows the results of reconstruction without the regularizing term (Fig. 5c) and with total variation regularization (Fig. 5d). In the image reconstructed without regularization Gibbs phenomena are notable. These effects are inevitable, since the phantom has infinite support in frequency domain, whereas the image is reconstructed from band-limited sampling.

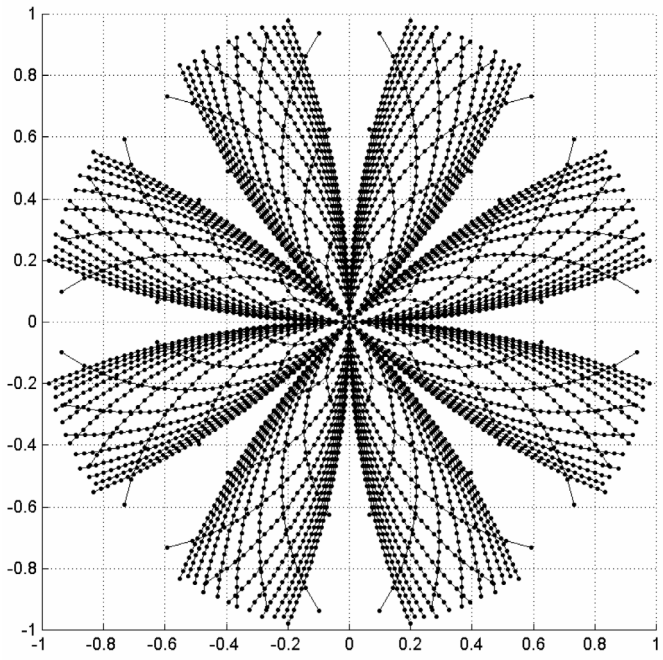

Fig. 4. Frequency domain sampling corresponding to 8 broadband projections (normalized spatial frequency).

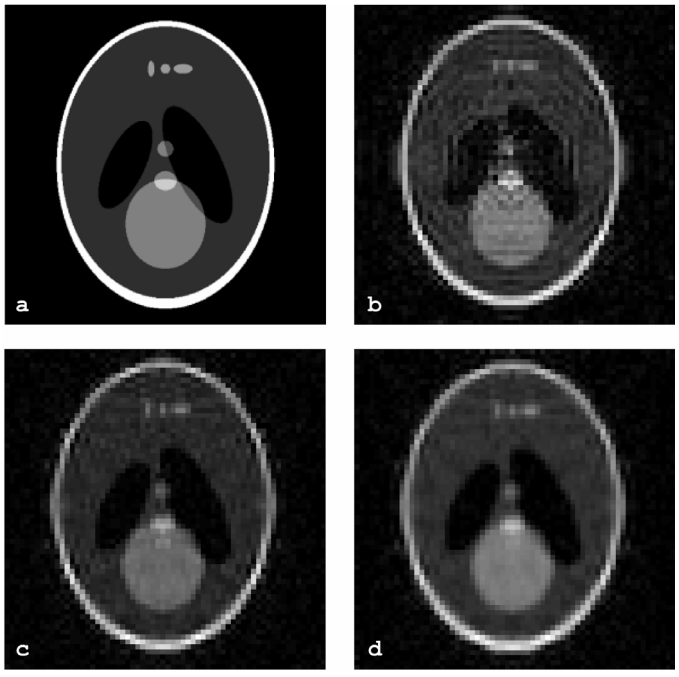

Fig 5. a. original band-unlimited phantom, b. reconstruction by gridding, c. iterative least-squares reconstruction, d. iterative reconstruction with total variation penalty (λ = 100).

[1] MATLAB code is available from http://www.eecs.umich.edu/~fessler courtesy of Jeffrey Fessler.

When introducing the total variation penalty term, small artifacts of oscillatory nature are first to disappear; however, too strong penalty is liable to affect small features of the image.

The influence of total variation regularization is especially significant in presence of noise. Since ultrasound images usually suffer from low SNR, this aspect is of high importance. Figure 7 shows images reconstructed from data contaminated by additive Gaussian noise with different variance. One can observe that the total variation penalty improves the image quality, whilst preserving the edges.

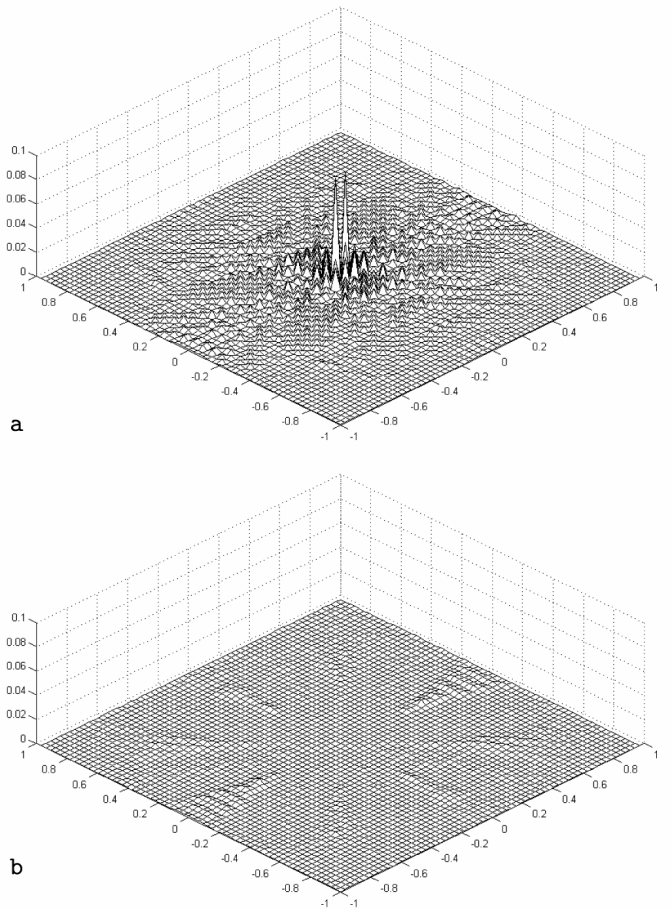

Fig. 6. Magnitude of error in frequency domain of an image reconstructed using gridding (a), and using NUFFT (b).

VI. Conclusions

We showed an iterative reconstruction algorithm based on min-max NUFFT for ultrasound tomography with diffracting sources. The presented method is capable of taking advantage of broadband illumination and requires fewer projections for image reconstruction. It appeared significantly more accurate compared to the common gridding method.

Total variation regularization further improves the image quality, suppressing noise and Gibbs phenomena, thus allowing obtain sufficient reconstruction quality from noisy data.

Possible developments of the iterative approach can be generalization of the regularizer for other classes of signals, incorporation of different NUFFT implementations and non-smooth optimization techniques for efficient minimization of functions with non-smooth penalty terms.

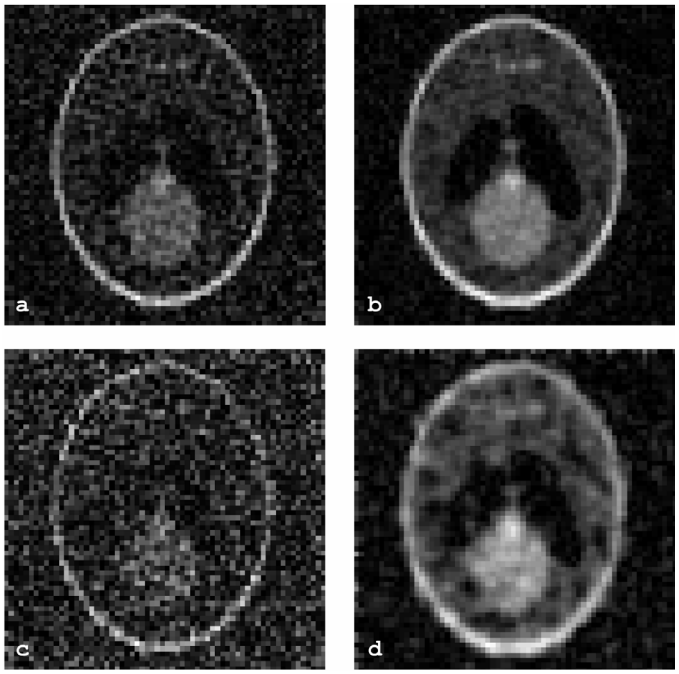

Fig. 7. Iterative reconstruction in presence of noise (a, b: SNR = 20dB, c, d: SNR = 10dB) with total variation penalty $\lambda = 100$ (b, d) and without penalty (a, c).

Acknowledgment

We are indebted to Jeffrey Fessler (The University of Michigan) who attracted our attention to his novel approach of NUFFT computation and kindly provided his code. We would also like to thank Haim Azhari and Yehoshua Y. Zeevi (Technion) for their valuable comments.

References

[1] A. C. Kak and M. Slaney, *Principles of Computerized Tomographic Imaging*, Society of Industrial and Applied Mathematics, 2001.

[2] G. Beylkin, "On the fast Fourier transform of function with singularities", *Applied and Computational Harmonic Analysis* 2, pp. 363-381, 1995.

[3] A. Dutt and V. Rokhlin, "Fast approximate Fourier transforms for nonequispaced data", *SIAM J. Sci. Comput.*, Vol. 14, No. 6, pp. 1368-1393, November 1993.

[4] A. Dutt and V. Rokhlin, "Fast approximate Fourier transforms for nonequispaced data II", *Applied and Computational Harmonic Analysis* 2, pp. 85-100, 1995.

[5] A. J. W. Duijndam and M. A. Schonewille, "Nonuniform fast Fourier transform", *Geophysics Online*, February 1999.

[6] J. Fessler and B. P. Sutton, "Non-uniform fast Fourier transforms using min-max interpolation", submitted to *IEEE Trans. Signal Processing*, 2001.

[7] J. Fessler, "Iterative tomographic image reconstruction using non-uniform fast Fourier transforms", 2001.

[8] P. Blomgren, T. F. Chan, P. Mulet and C. K. Wong, Total variation image restoration: numerical methods and extensions, Proc. ICIP 97.

[9] E. Jonsson, S. C. Huang and T. Chan, "Total Variation Regularization in Positron Emission Tomography", *CAM* 98-48, 1998, http://www.math.ucla.edu/~chan/papers.html

[10] P. Kisilev, M. Zibulevsky and Y. Y. Zeevi, "Total variation and wavelet regularization methods in emission tomography", Research Report, Technion – Israel Institute of Technology, 2001.
[11] F.T.A.W. Wajer, R. Lethmate, J.A.C. van Osch, D. Graveron-Demilly, M. Fuderer and D. van Ormondt, "Interpolation from arbitrary to Cartesian sample positions: gridding", Proceedings *ProRISC/IEEE Workshop*, 2000.
[12] D. P. Bertsekas, *Nonlinear Programming*, 2nd ed., Athena Scientific, 1999.
[13] S. Mallat, *A Wavelet Tour of Signal Processing*, 2nd ed., Academic Press, 1999.
[14] M. Bronstein, A. Bronstein and M. Zibulevsky, "Iterative reconstruction in diffraction tomography using NUFFT", Research Report, Department of Electrical Engineering, Technion - Israel Institute of Technology, 2002, http://visl.technion.ac.il/bron/works